Plastic behavior and shakedown limit of defected pressurized pipe under cyclic bending moment

Mark Nassef Naguib Youssef[1*], Mohammad Mohammad Megahed[1], Chahinaz Abdel Rahman Saleh[1] and Sahour Nabil Sayed Mohammed[1]

*Correspondence:
m.nasef.naguib@eng.cu.edu.eg

[1] Mechanical Design and Production Department, Faculty of Engineering, Cairo University, Cairo, Egypt

Abstract

Pipelines subjected to thermal or mechanical loads may fail due to plastic strain accumulation which leads to ratcheting**.** In this research, cyclic plastic behavior and shakedown limit are investigated experimentally and numerically for a defected pressurized pipe under cyclic bending moment. In the numerical model, the combined isotropic/kinematic hardening model based on the Chaboche model is adopted to represent the cyclic plastic flow of the material. The hardening parameters are determined experimentally and used in the finite element (FE) model. A four-point bending test rig is manufactured to test a pressurized API 5L steel pipe under cyclic bending. An elliptical defect is created by machining to depict corrosion pits in pipes. The plastic strains are measured experimentally and the results are used to tune the parameters of the FE model. The shakedown limit of the defected pipe is determined numerically by tracking the critical points behavior and the results are verified experimentally. Furthermore, the plastic work dissipated energy (PWD) is estimated within the defective structure to study the behavior of the pipe. By running this compatible model, it is found that the yield and the shakedown limits are lowered by mean values of 55% and 25% respectively due to the presence of metal loss defect occupying almost half of the pipe thickness.

Keywords: Ratcheting, Shakedown, Defected pipes, Plastic work dissipation, Cyclic moment

Introduction

The ratcheting effect is when the plastic deformation of a structure or material is accumulated if it is subjected to a steady primary load in the presence of a secondary cyclic load. Excessive strain cycles might lead mechanical components to fail if the strain exceeds the shakedown limit which leads to ratcheting. Within the past few decades, ratcheting failure was one of the main reasons for catastrophic disasters related to many structures, especially pipes [1, 2]. These unexpected failures happened mainly due to the presence of localized defects which act as stress risers.

Youssef *et al. Journal of Engineering and Applied Science* (2024) 71:106

Page 2 of 16

Pipes are essential components in most industries, such as power, nuclear, and petrochemical plants; oil and gas platforms; wind turbine towers; high-rise buildings and other applications [3]. In most of these applications, pipes are pressurized and subjected to cyclic thermal and/or mechanical loadings. After many years in service, corrosion defects appear leading to external and internal metal loss. These defects cause stress concentrations that may exceed the elastic limit of the pipe material when subjected to cyclic loads. This leads to structural ratcheting and if it continues it leads to leakage and failure of the pipe or other components connected to it.

Therefore, it is important to identify the ratcheting behavior of pipes under cyclic loading and develop methods to mitigate this phenomenon to prevent catastrophic failures and ensure the integrity and safety of the structure. While there have been extensive research efforts to understand and predict the ratcheting behavior of pipes, more work is still needed in this field. This is due to the fact that most studies are focused on intact pipes and components without considering the presence of defects or stress raisers. Another point to consider is, that the material modeling techniques for the ratcheting behavior is a tedious and lengthy task and require special arrangements and skills. Hence, the application of the newly developed SD_{lim}-PWD method [4] that deals with the characterization and prediction of ratcheting behavior in pipes with defects would greatly benefit the industry.

Literature review

In 1938, Melan introduced the shakedown theorem for materials that behave as elastic-perfectly plastic materials subjected to loads [5]. In 1967 [6], Bree analyzed the behavior of a pressurized cylinder subjected to cyclic thermal stresses through its wall thickness. He proposed the interaction diagram, which was later known as the Bree interaction diagram or Bree diagram. The Bree diagram shows the boundaries defining the different responses of a structure to the present loads. Pressure vessels and piping codes of practice such as ASME [7] and KTA [8] have adopted the Bree diagram to determine the shakedown and ratcheting limits. Bao et al. [9] discussed the mechanical models for a variety of uniaxial Bree-type situations. They have constructed shakedown boundaries under three different loading conditions. Based on 4D ratcheting boundary theory and numerical results, semi-analytical parametric equations of the shakedown boundaries are derived. Their results enhanced the understanding of pressure equipment structural behavior and provided guidance for ratcheting assessment and shakedown design of practical industrial components. Surmiri et al. [10] further studied the Bree problem. They have coupled the non-linear kinematic hardening of Chaboche with continuum damage mechanics to investigate the response of a hollow sphere subjected to cyclic thermal loadings and constant internal pressure. They illustrated a modified Bree diagram and it was shown that due to the developed damage, the plastic shakedown region diminishes.

Many methods that use FE analysis to determine the shakedown and ratcheting limits of structures assume the material to behave as elastic-perfectly plastic. Among these methods are the linear matching method (LMM) introduced by Chen and Ponter [11] which has been used in many studies [9, 12, 13] and the simplified technique developed by Abdalla et al. [14]. One of the limitations related to these methods is

Youssef *et al. Journal of Engineering and Applied Science* (2024) 71:106

Page 3 of 16

that they can only be used to study components undergoing small deformations. In 2021, Abdallah [4] proposed an approach to predict the shakedown limit given the history of plastic work dissipation. The approach is based on the idea that plastic work dissipation is proportional to plastic strain accumulation. The method introduces a series of elastic–plastic FE full cyclic loading simulations till the shakedown limit is found through monitoring the plastic work dissipation history.

Although there is a large number of studies that address the plastic behavior of sound-pressurized pipes subjected to the cyclic moment [15–17], and many studies that study defective elbows [18–20], there is a shortage in the researches that address the behavior of straight defected pipes. Pinheiro and Pasqualino [21] examined dented steel pipelines subjected to cyclic internal pressure, establishing analytical expressions to evaluate stress concentration factors based on damaged pipe geometric parameters. Chen et al. [22] used the LMM to study the effects of different dimensions and configurations of part-through slots within a pipe and presented shakedown and ratchet limit interaction diagrams. Chen and Chen [23] used FE analysis to examine the ratcheting behavior of stainless steel pressurized straight pipes under reversed cyclic bending with rectangular local wall thinning. Hamidpour and Nayebi [24] analyzed the elastic, plastic shakedown, and shakedown limits of defected pressurized pipelines under a cyclic thermal gradient. They found that the elastic and plastic shakedown domains may significantly decrease for certain defect configurations. Zeinoddini and Pekanyu [25] studied numerically the ratcheting behavior of cyclic axially loaded steel tubes with rectangular defects, observing the surface imperfections effect on ratcheting response. Jiang et al. [26] investigated mitred girth butt weld pipelines with crack defects through full-scale experiments and FE. They found out that circumferential burst failure appeared for defect-free mitred pipes, while the failure is longitudinal on cracked mitred pipes. Thin-walled steel pipes under cyclic internal pressure were studied experimentally and numerically by Karimi and Shariati [27]. They have shown that the ratcheting strain is mostly significant in the hoop direction of the pipe and that increasing the pressure amplitude and mean pressure increases the ratcheting strain percentage. Lourenco and Netto [28] studied ratcheting in pipes with axisymmetric and elliptical defects and demonstrated the effect of defect type and configuration on the shakedown limit.

Methods

In this research, a compatible numerical model based on experimental tests is presented. The model is used to study the plastic behavior and shakedown limit of defected pressurized pipes under cyclic bending moment. The 2-in. diameter API 5L Schedule 40 pipe mechanical properties are imported in the numerical model. The Chaboche model presented in ABAQUS software is utilized to simulate the cyclic plastic behavior of the pipe material. Pipes with a single elliptical defect at the outer surface are tested experimentally under prescribed loads using a manufactured test rig. The results obtained from the tests are used to calibrate the material hardening parameters used in the FE model. The FE model is then used to determine the shakedown limit by studying the strain field at the critical points and estimating the dissipated plastic energy of the whole structure.

Youssef *et al. Journal of Engineering and Applied Science* (2024) 71:106

Page 4 of 16

Finite element modeling

The FE model for the pressurized defected pipe under cyclic bending moment is developed to predict the shakedown limit for the addressed pipe. ABAQUS software (version 6.14) is used in the FE analysis, and the built-in Chaboche hardening model is used to model the cyclic plastic behavior of the material. Experimental test results (monotonic tension, cyclic tension, and four-point bending tests) are used to get the hardening parameters of the Chaboche model.

The problem is solved using the standard solver. To minimize the solution time of the numerical model, symmetry in both the longitudinal and transverse planes is assumed and one-quarter of the pipe is modeled. The pipe is restricted to move at the symmetry planes, while it is allowed to move freely at the loaded end and radially. The pipe is modeled as a 3D quarter pipe with the same dimensions as the original pipe. The 3D model is been chosen due to the shape and geometry of the defect, which are hard to be properly presented in a shell model. The defect is created by removing the metal loss from the modeled pipe and partitions are created in the model to facilitate structural meshing as shown in Fig. 1.

The material properties such as Young's modulus of elasticity, Poisson's ratio, and hardening parameters which are obtained experimentally and given in detail in further sections are used to define the pipe material. The loading procedure is composed of two steps similar to the experimental setup. At the beginning, the pressure is applied to the interior surface of the pipe through a ramp function and when the target value is reached, it is then maintained and the cyclic bending moment is applied. In order to apply the moment to the pipe, a moment around the *x*-axis is applied to a reference point connected to the solid end of the pipe through a coupling. The moment step has 100 steps with an increment size of 0.1 representing the 100 cycles of the moment. The amplitude of the moment is included in the definition of the moment.
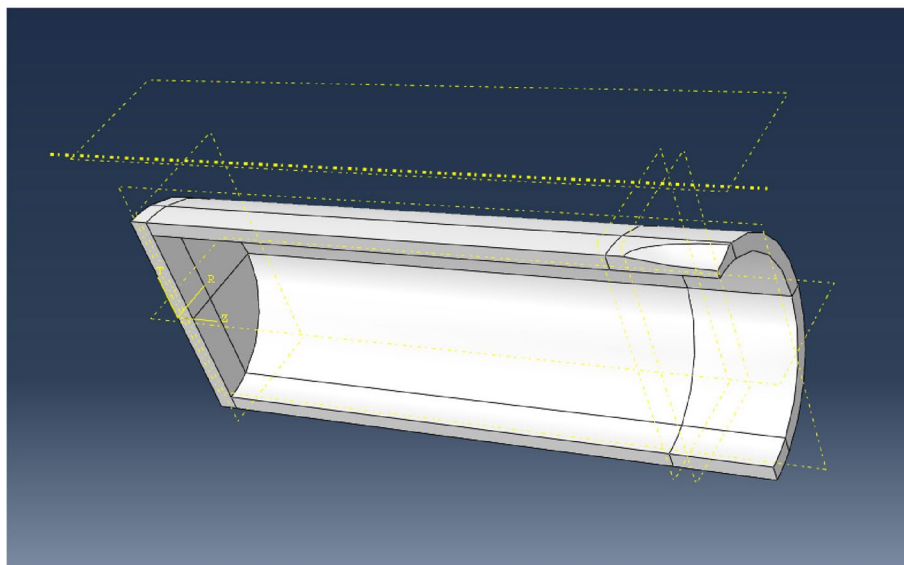

Fig. 1 FE model of the defective pipe

Youssef *et al. Journal of Engineering and Applied Science*   (2024) 71:106

Page 5 of 16

The meshing is done through using of three-dimensional quadratic solid brick elements with 20 nodes and 8 integration points. Overall, 3039 quadratic hexahedral elements of type C3D20R represent the studied model as shown in Fig. 2. The element at the defect center (where maximum strain is located) on the external surface is used to obtain the reading of the strain that was compared to the experimental results. The average value of the integration points on the surface of this element was used to produce more accurate results. A sensitivity analysis was performed to determine the acceptable element size within the defect zone, and the strain gauge was selected to be of the same size as the chosen element, allowing for the results to be more relatable between the numerical model and the experiment.

Calibration of the FE model

To have a compatible model, the material model parameters used in FE are determined experimentally prior to conducting the numerical analyses. The pipe material used in this study experiences hardening with loading cycles where the flow stress increases with each cycle compared to the initial half-cycle. In order to define the material behavior, the stress–strain data of the first half cycle of the uniaxial tension test is used as an input in the FE software [29].

Combined hardening material models are introduced as an alternative to bilinear models to better represent material behavior. For instance, the isotropic hardening model describes a yield surface that changes its size while having its center at the same location. On the other hand, kinematic hardening models describe a yield surface without a change in size while the location is changing. In the present work, the Chaboche model, which is a combined hardening model, is applied to enhance the accuracy of the analysis where the size of the yield surface and its center change
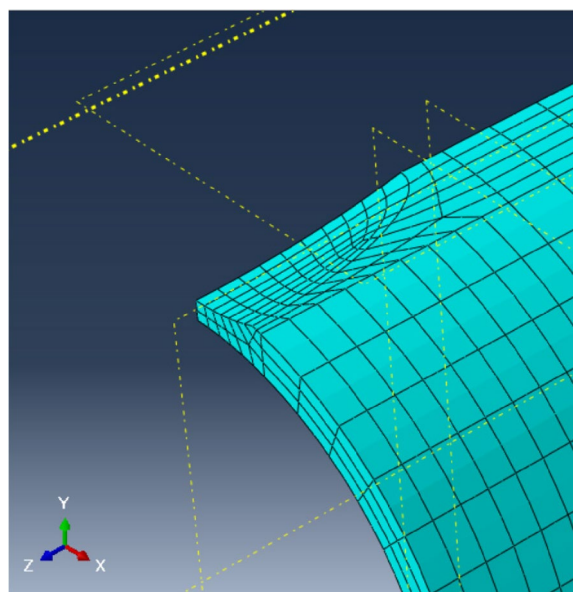

Fig. 2 3D meshes of the defected pipe

during the cyclic plastic deformation. The difference between isotropic, kinematic, and combined models is illustrated in Fig. 3.

Determination of the hardening parameters

The Chaboche hardening model is a combined isotropic and kinematic hardening model. The isotropic hardening flow stress in relation to the deformation is found to be: [31]

$$\sigma = \sigma_0 + Q\left(1 - \exp\left(-b\frac{\Delta\varepsilon_p}{2}\right)\right)$$

Where σ_0 is the yield stress at zero plastic strain, ε_p is the plastic strain, "Q" and "b" are representing isotropic hardening in the model where "Q" describes the maximum change in the size of the yield surface, and "b" describes the rate of yield surface size change with plastic strain.

The isotropic hardening coefficients are calculated from the experimental data obtained from the monotonic tensile test. As a result, the hardening coefficients Q and b were found to be 97 MPa and 7 MPa, respectively.

For kinematic hardening, the movement of the center of the yield surface depends on the plastic flow, and its location is defined by the parameter (α) according to the following relation: [31]

$$\alpha_k = \frac{C_k}{\gamma_k}(1 - e^{-\gamma_{kg^{pl}}})$$

where "α_k" is the backstress or the kinematic shift of the yield locus, the coefficients "C_k" and "γ_k" are the kinematic hardening parameters, and the subscript "k" is the number of the Chaboche parameters chosen for the analysis. The approach proposed by Kalnins et. al [32] is followed for determining these parameters. This approach is based on the monotonic stress–strain curve of a tensile specimen where it is expected that it will yield cautious predictions of ratcheting, which would be deemed acceptable for design reasons. This is due to the fact that the flow stress increases with each subsequent cycle, surpassing that of the initial half-cycle. This phenomenon is observed in steels, as discussed in this work. The number of the Chaboche parameters (k) is left to the choice of the analyst. In this study, only three Chaboche parameters are chosen and their initial values which are shown in Table 1 are calculated. These values are then calibrated based on matching the uniaxial stress–strain data with the backstress curve and the calibrated values are shown in Table 2.

Experimental

Pipe material and dimensions

The considered pipe in this study is API 5L low carbon steel, having 38 mm outside radius (R_0), 3.9 mm thickness (t), and length (l) of 700 mm. Standard tensile specimens based on the ASTM E8 [33] are cut from the pipe. The true stress–strain curve obtained from the test is shown in Fig. 4, and the material mechanical properties are presented in Table 3. These stress–strain data were used as input data in ABAQUS for the definition of the material behavior using the half-cycle option.
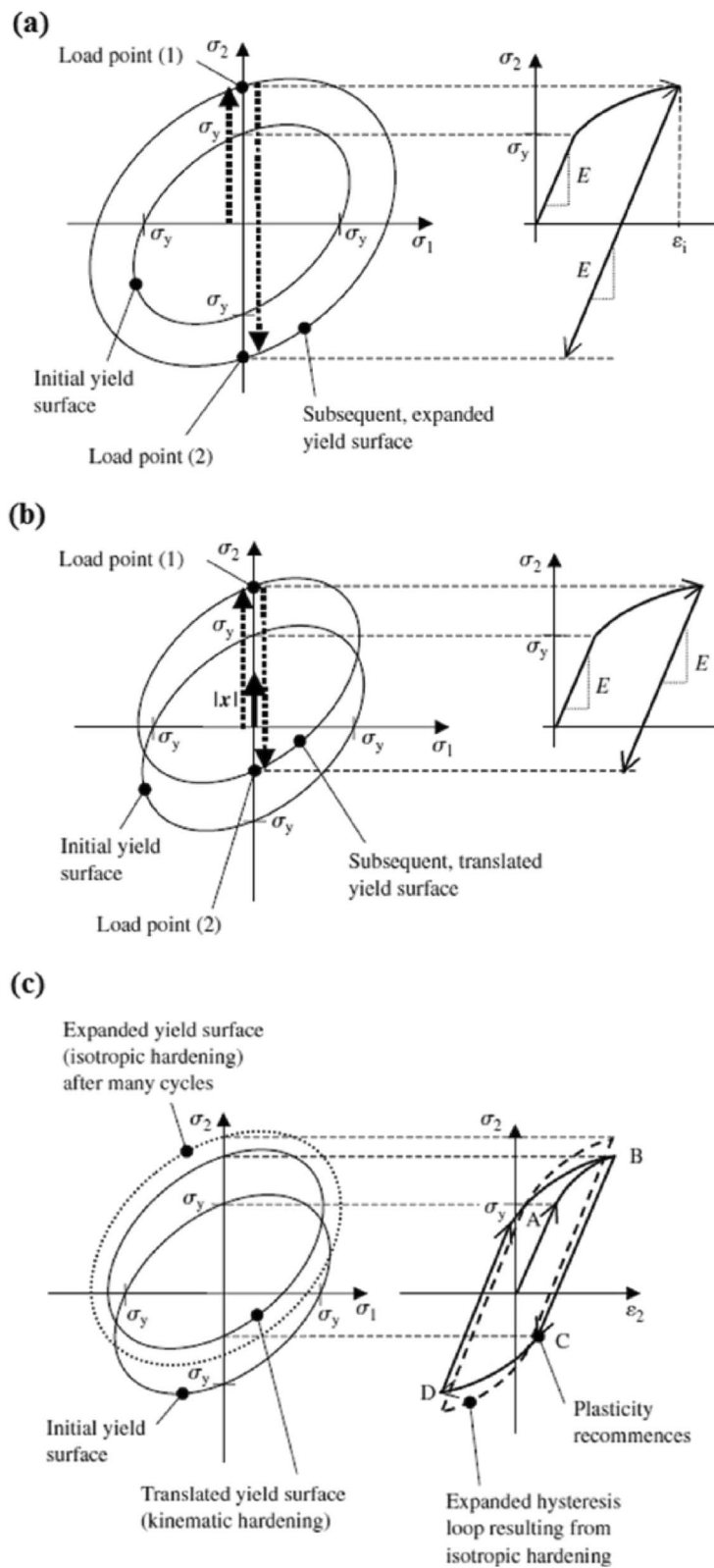
Fig. 3 Material behavior under cyclic loading based on isotropic hardening (**a**), kinematic hardening (**b**), and mixed hardening (**c**) [30]

Youssef *et al. Journal of Engineering and Applied Science*   (2024) 71:106

Page 8 of 16

Table 1 Initial values for the Chaboche parameters

Chaboche component	C MPa	γ
Parameter 1	65,000	666.67
Parameter 2	54,289.47	500
Parameter 3	1110.526	25

Table 2 Calibrated values for the Chaboche parameters

Chaboche component	C MPa	γ
Parameter 1	58,120	826
Parameter 2	48,567	580
Parameter 3	1723	2.5
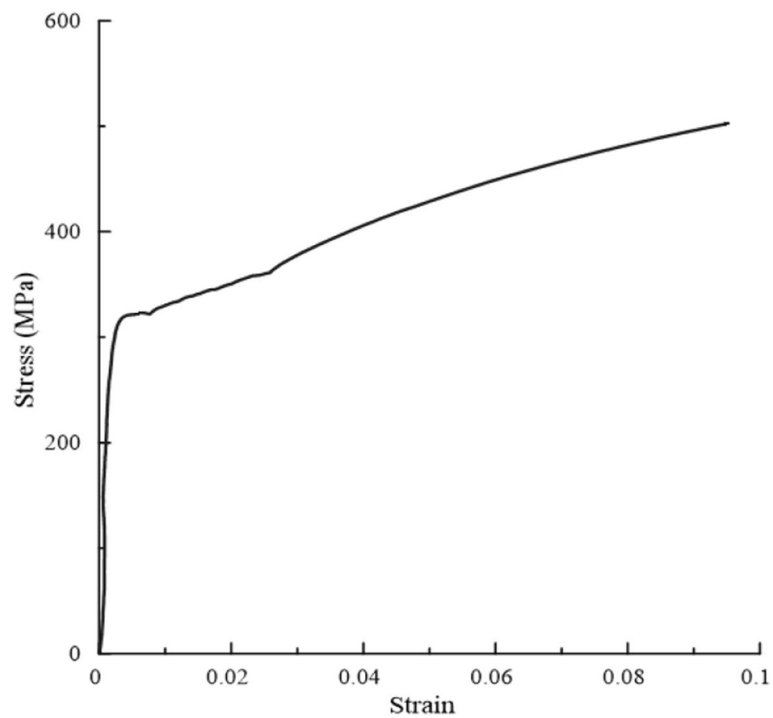
Fig. 4 True stress–strain curve of the API 5I pipes material

Table 3 Mechanical properties of API 5I pipes material

Material property	Value
Yield stress (σ_0) at 0.2% offset	308 MPa
Ultimate stress (σ_{ult})	502 MPa
Poisson's ratio (υ)	0.28
Young's modulus of elasticity (E)	186 GPa
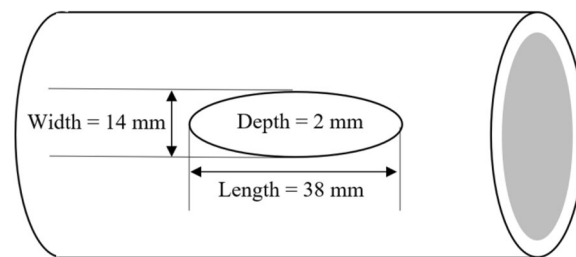
Fig. 5 Defect configuration on the outer surface of the pipe
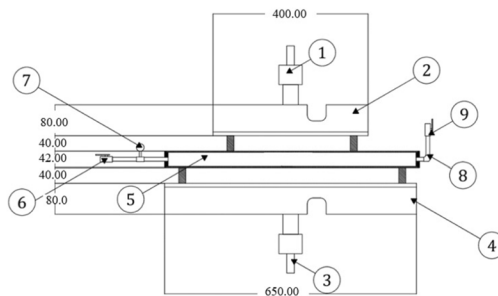
Item No.	Part Name
1	Upper Grip
2	Upper Support
3	Lower Grip
4	Lower Support
5	Pipe
6	Inlet Valve
7	Pressure Gauge
8	Outlet Pipe
9	Outlet Valve
10	U-Support Rings

Fig. 6 Schematic drawing of the 4-point bending test rig

Defect configuration

An elliptical defect is machined in the middle of the cylinder with a width of 14 mm ($= 0.3 R_0$), and a length of 38 mm ($= R_0$). and a depth of 2 mm ($= 0.52$ t); the defect configuration is shown in Fig. 5

Test rig and experimental setup

A four-point bending test rig is designed and manufactured to apply pure bending moment on the middle zone of the pipe, as shown in Fig. 6. The pipe is smoothly supported at four locations on the stiff lower and upper loading beams with 100 mm side distance between the supports on each side. Rings of circular cross-section are used to support the pipe to allow the relative axial movement of the pipe and produce vertical reactions upon loading. The test rig is attached to a universal testing machine, and the cyclic vertical movement of the head bends the pipe according to the program of loading. The pressure is applied using a manual hydraulic pump and the pressure inside the pipe is monitored through a pressure gauge. The pipe during the experiment is subjected to a bi-axial state of stress resulting from the internal pressure, and secondary axial stress from the cyclic bending, as shown in Fig. 7. In order to measure the strain, two strain gauges of size 5 mm are fixed to the pipe where they are aligned to the hoop and axial directions, as illustrated in Fig. 8. The measurements of strain are conducted using Kyowa PCD-300a strain-meter.

Results and discussion

Using the FE analysis with the internal pressure (P_0), it is found that the pressure causing yielding is 48 MPa and the moment that causes yield (M_0) is found to be 2.1 kNm. To be able to verify the FE model using the "Shakedown Limit–Plastic Work
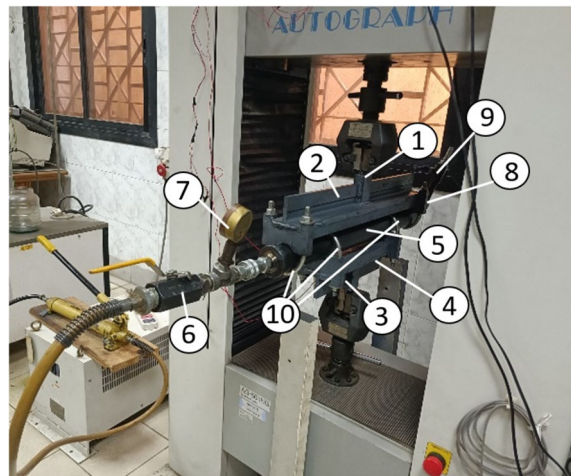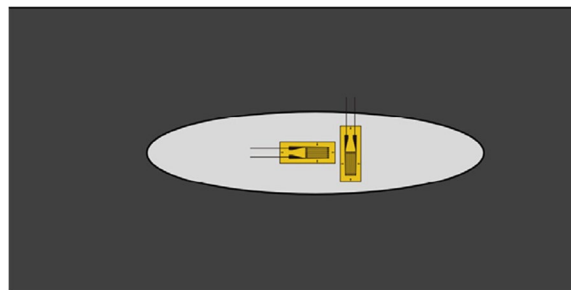
Fig. 7 Experimental setup

Fig. 8 Strain gauges position at the defect on the surface of the pipe

Table 4 Load boundary conditions used to verify the FE model

Boundary conditions	Case 1	Case 2
Internal pressure	0.25 P_0 (12 MPa)	0.25 P_0 (12 MPa)
Max. bending moment	0.85 M_0 (1.78 kN m)	0.7 M_0 (1.47 kN m)
Min. bending moment	0.085 M_0 (0.178 kN m)	0.07 M_0 (0.147 kN m)

Dissipation" (SD_{LIM}−PWD) method, two cases are tested experimentally and compared to the FE model. The pressure and moment values used for the two cases are shown in Table 4.

Since the change in the plastic work dissipation (PWD) is directly related to the generated equivalent plastic strain, then the unchanged PWD means that the structure is in the shakedown state, while the accumulation of PWD indicates the ratcheting state. For a pressurized pipe, the cyclic bending moment is applied with a magnitude higher than that causing yielding and the PWD is checked during loading. If the PWD is accumulating, we lower the value of the moment gradually till the accumulation disappears, and we define this as the shakedown limit. If the PWD is not accumulating, we increase the value gradually till accumulation happens, and we

define this as the shakedown limit. We check the PWD for the first 100 cycles to show if the accumulation is happening or not, and based on the different load combinations we can determine the shakedown limit for the whole structure.

The presence of the defect increases the stress level at the lowest point of the defect, as shown in Fig. 9. The variation of measured strains with the loading cycles in both the axial and hoop directions at the defect location as well as the strains obtained from the FE analysis are plotted for both loading cases as shown in Figs. 10 and 11. In addition, the total plastic work dissipated for each case is numerically estimated as shown in Figs. 12 and 13.

The two loading scenarios show a clear distinction between the ratcheting and shakedown behaviors. It appears in the ratcheting case, that increasing the range of moment while maintaining the pressure at the same value leads to accumulation in plastic strain, while the strain reaches a steady value for the smaller moment range leading to shakedown. Based on the comparison between hoop and axial strains obtained experimentally and those obtained using the FE model, an acceptable agreement is found with a maximum difference of 5%.

The plastic work dissipation in both cases confirms these results but in a more holistic way, where the whole body is looked at. The accumulation in energy is shown in the case of ratcheting as compared to the shakedown case. The incremental accumulation of the PWD indicates that the pipe is operating beyond the shakedown limit. On the other hand, PWD in the shakedown case is constant, as there is no accumulation of the strain, which means that the pipe is operating below the shakedown limit.

Based on the previously presented results, the FE model is verified. The model is then used to obtain the interaction diagram for the same pipe. In order to obtain the
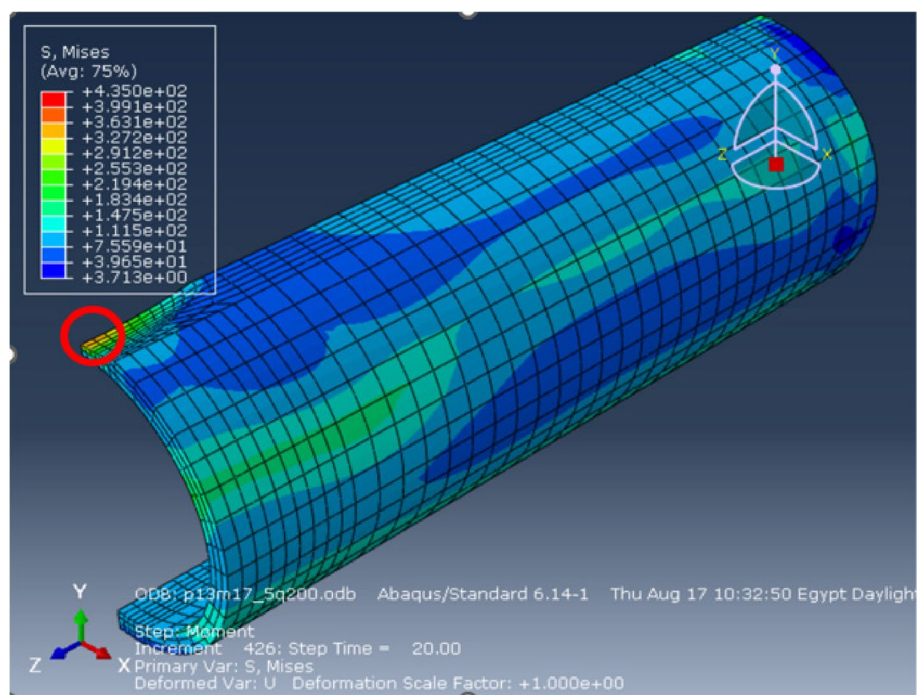

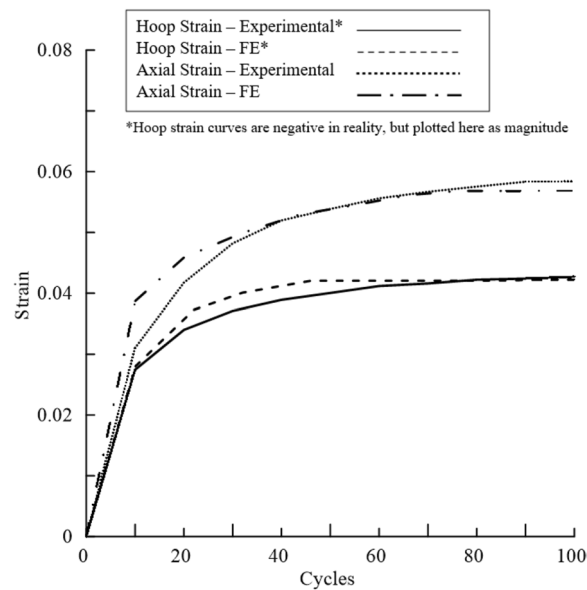**Fig. 9** FE model showing the location of maximum Mises stress at the center of the defect

Fig. 10 Axial and hoop strain at the defect center, case 1 (ratcheting) ($M = 0.85M_0$ and $P = 0.25P_0$)
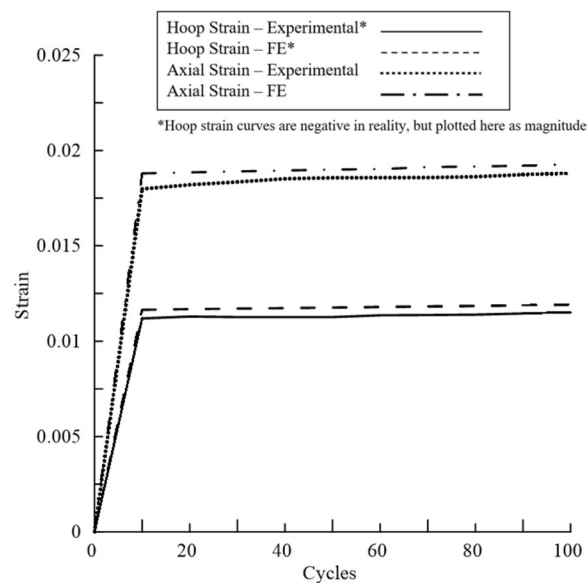

Fig. 11 Axial and hoop strain at the defect center, case 2 (shakedown) ($M = 0.7M_0$ and $P = 0.25P_0$)

interaction diagram, the elastic limits for both the intact and the defective pipes are plotted as presented in Fig. 14. Different load combinations were simulated for both the intact and defective pipes. The behavior is considered shakedown or ratcheting based on the plastic work dissipation curve for each case.

The presence of the defect has reduced the yield limit dramatically to a mean value of 55% of the intact pipe as can be shown in Fig. 14. The different load combinations in terms of pressure and moment produce different behaviors of the pipe. Although the yield is exceeded at many points, the shakedown behavior can be observed for
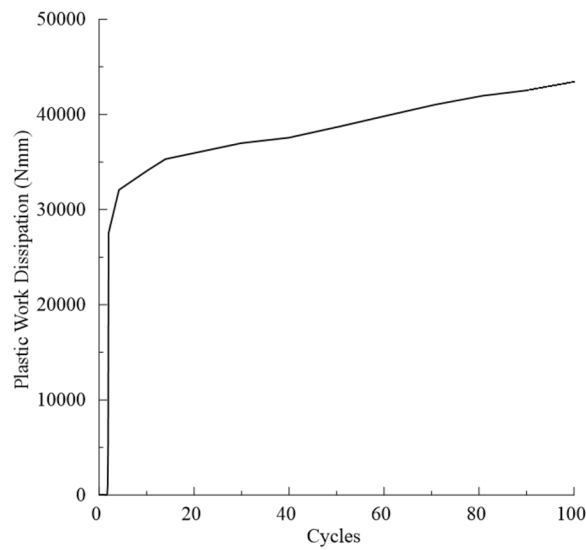
Fig. 12 Plastic work dissipation during loading cycles, case 1 (ratcheting) ($M = 0.85\,M_0$ and $P = 0.25P_0$)
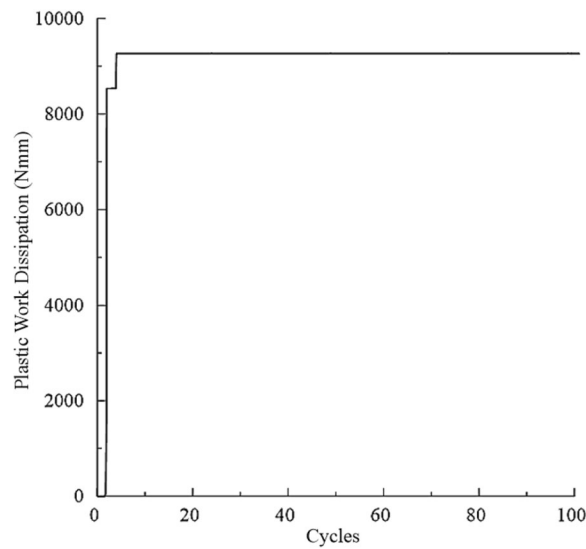

Fig. 13 Plastic work dissipation during loading cycles, case 2 (shakedown) ($M = 0.7\,M_0$ and $P = 0.25P_0$)

much higher load combinations. This means that the defective pipe can be still used even if the load exceeds the yield limit. It can also be noticed that the presence of defect has decreased the shakedown/ratcheting limit to a mean value of 25%. of the intact pipe shakedown/ratcheting limit. This can be seen when we compare different points on the shakedown limit for the intact pipe versus the defective pipe. It is worth mentioning that the plotted diagram is limited to the material, size, and defect configuration addressed in this research.
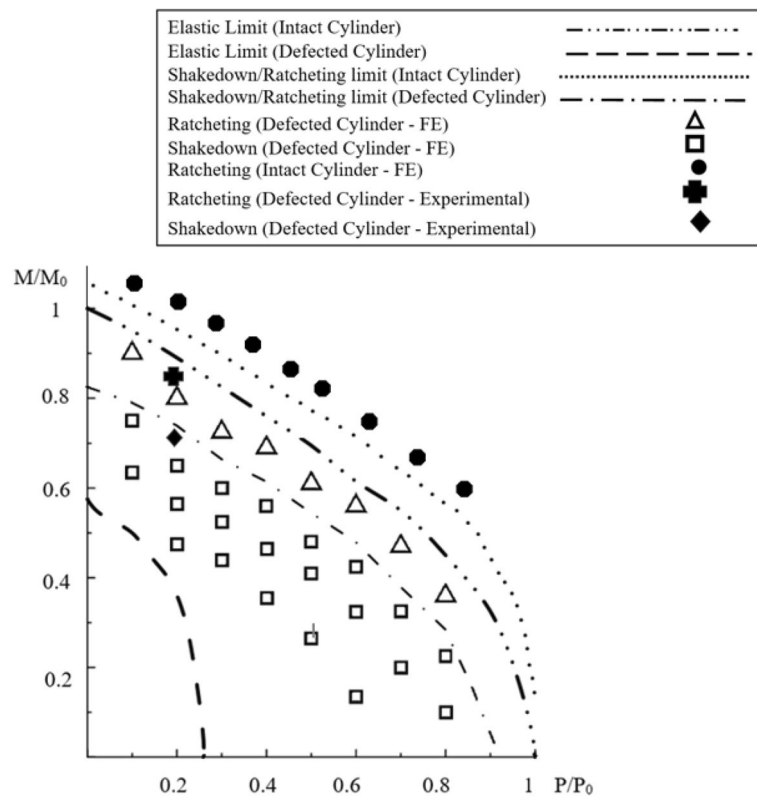
Fig. 14 Interaction diagram for the intact and defective pipe

Conclusions

This study has successfully addressed several crucial aspects related to the testing and analysis of pressurized defective pipes using a simplified approach. The plastic cyclic behavior of the pipe is predicted with an accuracy of 95% by implementing the experimental stress–strain data in FE analysis.

The application of the plastic work dissipation approach has demonstrated its efficiency in predicting both shakedown and ratcheting behaviors and aligning the results close to the experimental strain results could optimize both time and effort.

The presence of a highly strained region within the defect highlights the pivotal role played by defects in the pipe's structural response. The developed interaction diagram can show the load combinations that lead to shakedown or ratcheting and the limit between both regions can be found as well.

Future research will be focused on exploring the impact of different defect dimensions, configurations, and the interaction of multiple defects. These investigations could provide deeper insights into the broader spectrum of pipe behavior under various conditions.

Abbreviations
B Hardening coefficient describes the change rate of yield surface size during plastic strain
E Young's modulus of elasticity
FE   Finite element
L Pipe length
LMM   Linear matching method

M_o	Yield moment of intact pipe
P_o	Yield pressure of intact pipe
PWD	Plastic work dissipation
Q	Hardening coefficient describes the largest size change of the yield surface during plastic strain
R_o	Pipe outer radius
SD	Shakedown
SD_{lim}	Shakedown limit
T	Thickness of the pipe
ε_p	Plastic strain
σ_0	Yield stress at zero plastic strain
σ_{ult}	Ultimate stress
υ	Poisson's ratio

Declarations

Competing interests
The authors declare that they have no competing interests.

References

1. Salge M, Milling P (2006) Who is to blame, the operaor or the designer? Two stages of human failure I the Chernobyl accident. Sys Dynamic Review 22:89–112
2. Sovacool BK (2008) The costs of failure: a preliminary assessment of major energy accidents, 1907–2007. Energy Policy 36:1802–1820. https://doi.org/10.1016/j.enpol.2008.01.040
3. Aswin A, Hasnan A (2023) Stress analysis evaluation and pipe support type on high-pressure and temperature steam pipe. Int J Mech Eng Technol Appl 4:31–38. https://doi.org/10.21776/mechta.2023.004.01.4
4. Abdalla HF (2021) A novel methodology for determining the elastic shakedown limit loads via computing the plastic work dissipation. Int J Press Vessels Piping 191. https://doi.org/10.1016/j.ijpvp.2021.104327
5. Melan E (1938) Zur Plastizität des räumlichen Kontinuums. Ing. Arch 9:116–126. https://doi.org/10.1007/BF02084409
6. Bree J (1967) Elastic-plastic behaviour of thin tubes subjected to internal pressure and intermittent high-heat fluxes with application to fast-nuclear-reactor fuel elements. J Strain Anal 2:226–238. https://doi.org/10.1243/03093247v023226
7. (ASME), A.S.o.M.E., ASME Boiler and Pressure Vessel Code. Division1, Section III ; 2017.
8. KTA 3201.2 (2017) Components of the Reactor Coolant Pressure Boundary of Light Water Reactors—Part 2: Design and Analysis; Nuclear Safety Standards Commission (KTA): Salzgitter, Germany, pp. 1–162
9. Bao H, Shen J, Liu Y, Chen H (2022) Shakedown analysis and assessment method of four-stress parameters Bree-type problems. Int J Mech Sci 229. https://doi.org/10.1016/j.ijmecsci.2022.107518
10. Surmiri A, Nayebi A, Rokhgireh H (2018) Shakedown-ratcheting analysis of Bree's problem by anisotropic continuum damage mechanics coupled with nonlinear kinematic hardening model. Int J Mech Sci 137:295–303. https://doi.org/10.1016/j.ijmecsci.2018.01.030
11. Chen H, Ponter ARS (2001) A method for the evaluation of a ratchet limit and the amplitude of plastic strain for bodies subjected to cyclic loading. In Eur J Mech A/Solids 20
12. Chen X, Zhuang K, Zhu X, Chen H (2021) Limit load, shakedown and ratchet analysis of pressurized lateral nozzle. Smart Struct Syst 27:421–434
13. Choi Y, Cho NK, Yang J, Yun H, Lee H, Huh NS (2022) Shakedown and limit analyses of a pressurised water reactor vessel nozzle under cyclic thermo-mechanical loadings. Nucl Eng Des 397. https://doi.org/10.1016/j.nucengdes.2022.111947
14. Abdalla HF, Megahed MM, Younan MYA (2007) A simplified technique for shakedown limit load determination. Nucl Eng Des 237:1231–1240. https://doi.org/10.1016/j.nucengdes.2006.09.033
15. Gavriilidis I, Karamanos SA (2022) Structural response of steel lined pipes under cyclic bending. Int J Solids Struct 234–235. https://doi.org/10.1016/j.ijsolstr.2021.111245

16. Chen X, Tian Y, Liu S, Lang L, Zhu L (2022) Ratcheting evaluation of pressurized straight pipe using Ahmadzadeh–Varvani hardening rule. Thin-Walled Struct 179. https://doi.org/10.1016/j.tws.2022.109684

17. Saghi SG, Shariati M (2023) Experimental and numerical investigation of ratcheting behavior of SS316L seamless straight pipe under cyclic internal pressure and in-plane cyclic bending. Int J Press Vess Piping 205. https://doi.org/10.1016/j.ijpvp.2023.104996

18. Moradi A, Shariati M, Zamani P, Karimi R (2023) Experimental and numerical analysis of ratcheting behavior of A234 WPB steel elbow joints including corrosion defects. Proc Instit Mech Eng Part L: J Mater Des Appl 237:451–468. https://doi.org/10.1177/14644207221115517

19. Salehi A, Rahmatfam A, Zehsaz M (2022) Ratcheting assessment of corroded elbow pipes subjected to internal pressure and cyclic bending moment. J Strain Anal Eng Des 57:47–60. https://doi.org/10.1177/0309324721989897

20. Kamel Abbasnia S, Shariati M (2023) Experimental and numerical investigation of ratcheting behavior in seamless carbon steel 90° elbow pipe with small dimensions under constant internal pressure and in-plane cyclic bending. Int J Press Vessels Piping 204. https://doi.org/10.1016/j.ijpvp.2023.104974

21   Pinheiro B de C, Pasqualino IP (2009) Fatigue analysis of damaged steel pipelines under cyclic internal pressure. Int J Fatigue 31:962–973. https://doi.org/10.1016/j.ijfatigue.2008.09.006

22. Chen H, Chen W, Li T, Ure J (2012) On shakedown, ratchet and limit analyses of defective pipeline. J Press Vessel Technol Transact ASME 134. https://doi.org/10.1115/1.4004801

23. Chen X, Chen X (2016) Study on ratcheting effect of pressurized straight pipe with local wall thinning using finite element analysis. Int J Press Vessels Pip 139–140:69–76. https://doi.org/10.1016/j.ijpvp.2016.03.005

24. Hamidpour M, Nayebi A (2014) Elastoplastic analysis of defective pipelines under constant internal pressure and cyclic thermal loading. The 22st Annual International Conference on Mechanical Engineering-ISME2014

25. Zeinoddini M, Peykanu M (2011) Strain ratcheting of steel tubulars with a rectangular defect under axial cycling: a numerical modeling. J Constr Steel Res 67:1872–1883. https://doi.org/10.1016/j.jcsr.2011.05.010

26. Jiang J, Zhang H, Zhang D, Ji B, Wu K, Chen P, Sha S, Liu X (2022) Fracture response of mitred X70 pipeline with crack defect in butt weld: Experimental and numerical investigation. Thin-Walled Struct 177. https://doi.org/10.1016/j.tws.2022.109420

27. Karimi R, Shariati M (2020) Experimental and numerical analysis of ratcheting behavior of SS 316 L thin-walled pipes subjected to cyclic internal pressure. J Press Vessel Technol Transact ASME 142. https://doi.org/10.1115/1.4047652

28. Lourenço MI, Netto TA (2015) Ratcheting of corroded pipes under cyclic bending and internal pressure. Int J Press Vessels Pip 125:35–48. https://doi.org/10.1016/j.ijpvp.2014.09.002

29. Kubaschinski P, Gottwalt A, Tetzlaff U, Altenbach H, Waltz M (2022) Calibration of a combined isotropic-kinematic hardening material model for the simulation of thin electrical steel sheets subjected to cyclic loading. Materwiss Werksttech 53:422–439. https://doi.org/10.1002/mawe.202100341

30. Teimouri R, Amini S, Guagliano M (2019) Analytical modeling of ultrasonic surface burnishing process: Evaluation of residual stress field distribution and strip deflection. Mater Sci Eng, A 747:208–224. https://doi.org/10.1016/j.msea.2019.01.007

31. Baharom MH, Nikbakht E, Chatziioannou K (2023) Combined hardening parameters of high strength steel under low cycle fatigue. Eng Solid Mech 11:35–40. https://doi.org/10.5267/j.esm.2022.10.001

32. Kalnins A, Rudolph J, Willuweit A (2013) Using the Nonlinear Kinematic Hardening Material Model of Chaboche for Elastic-Plastic Ratcheting Analysis, ASME 2013 Pressure Vessels and Piping Conference

33. ASTM Standard E8/E8 M (2022) Standard test methods for tension testing of metallic materials. https://doi.org/10.1520/E0008_E0008M-22

Publisher's Note